Unusual electromagnetic scattering by cylinders of topological insulator

Lixin Ge,[1] **Tianrong Zhan,**[1] **Dezhuan Han,**[1,3,4] **Xiaohan Liu,** [1,2] **and Jian Zi**[1,2,*]

[1]*Department of Physics, Key laboratory of Micro and Nano Photonic Structures (Ministry of Education), and Key Laboratory of Surface Physics, Fudan University, Shanghai 200433, China*

[2]*Collaborative Innovation Center of Advanced Microstructures, Nanjing 210093, China*

[3]*Department of Applied Physics, Chongqing University, Chongqing 400044, China*

[4]*dzhan@cqu.edu.cn*

[*]*jzi@fudan.edu.cn*

Abstract: Topological insulators (TIs) show unusual optical responses resulting from a topological magnetoelectric (TME) effect. In this paper, we study theoretically the scattering of electromagnetic waves by circular TI cylinders. In certain configurations, the bulk scattering can be suppressed, leading to strong scattering in the backward direction in both Rayleigh and Mie scattering regimes due to the TME effect. At antiresonances, an interesting filed trapping phenomenon is found which is absent in conventional dielectric cylinders.

© 2014 Optical Society of America

OCIS codes: (160.4760) Optical properties; (290.4020) Mie theory; (260.5740) Resonance.

References and links

1. X. L. Qi and S. C. Zhang, "Topological insulators and superconductors," Rev. Mod. Phys. **83**, 1057–1110 (2011).
2. M. Z. Hasan and C. L. Kane, "Topological insulators," Rev. Mod. Phys. **82**, 3045–3067 (2010).
3. X. L. Qi, T. L. Hughes, and S. C. Zhang, "Topological field theory of time-reversal invariant insulators," Phys. Rev. B. **78**, 195424 (2008).
4. F. Wilczek, "Two applications of axion electrodynamics," Phys. Rev. Lett. **58**, 1799–1802 (1987).
5. X. L. Qi, R. D. Li, J. D. Zang, and S. C. Zhang, "Inducing a magnetic monopole with topological surface states," Science **323**, 1184–1187 (2009).
6. W. K. Tse and A. H. MacDonald, "Giant magneto-optical kerr effect and universal faraday effect in thin-film topological insulators," Phys. Rev. Lett. **105**, 057401 (2010).
7. W. K. Tse and A. H. MacDonald, "Magneto-optical faraday and kerr effects in topological insulator films and in other layered quantized Hall systems," Phys. Rev. B **84**, 205327 (2011).
8. J. Maciejko, X. L. Qi, H. D. Drew, and S. C. Zhang, "Topological quantization in units of the fine structure constant," Phys. Rev. Lett. **105**, 166803 (2010).
9. M. C. Chang and M. F. Yang, "Optical signature of topological insulators," Phys. Rev. B **80**, 113304 (2009).
10. J. Inoue, "An optical test for identifying topological insulator thin films," Opt. Express **21**, 8564 (2013).
11. X. Xiao, S. Li, K. T. Law, B. Hou, C. T. Chan, and W. J. Wen, "Thermal coherence properties of topological insulator slabs in time-reversal symmetry breaking fields," Phys. Rev. B **87**, 205424 (2013).
12. C. F. Bohren and D. R. Huffman, *Absorption and Scattering of Light by Small Particles* (John Wiley and Sons, 1983).
13. P. Sheng, *Introduction to Wave Scattering, Localization and Mesoscopoic Phenomena* (Springer-Verlag, 2006).
14. T. Ochiai, "Theory of light scattering in axion electrodynamics," J. Phys. Soc. Japan **81**, 094401 (2012),
15. L. X. Ge, T. R. Zhan, D. Z. Han, X. H. Liu, and J. Zi, "Determination of the quantized topological magneto-electric effect in topological insulators from Rayleigh scattering", arXiv:1404.2384 (2014).
16. I. V. Lindell, A. H. Sihvola, S. A. Tretyakov, and A. J. Viitanen, *Electromagnetic Waves in Chiral and Bi-Isotropic Media* (Artech House, 1994).

#223523 - $15.00 USD Received 19 Sep 2014; revised 8 Nov 2014; accepted 20 Nov 2014; published 4 Dec 2014
(C) 2014 OSA

17. B. N. Wang, J. F. Zhou, T. Koschny, M. Kafesaki and C. M. Soukoulis, "Chiral metamaterials: simulations and experiments," J. Opt. A: Pure Appl. Opt. **11**, 114003 (2009).
18. L. W. Zeng, R. X. Song, and X. L. Jian "Scattering of electromagnetic radiation by a time reversal perturbation topological insulator circular cylinder," Mod. Phys. Lett. B **27**, 1350098 (2013).
19. M. Akhtar, N. A. Naz, M.A. Fiaz, and Q. A. Naqvi "Scattering from topological insulator circular cylinder buried in a semi-infinite medium," J. Mod. Opt. **61**, 697–702 (2014).
20. M. Kerker, D.-S. Wang, and C. L. Giles, "Electromagnetic scattering by magnetic spheres," J. Opt. Soc. Am. **73**, 765–767 (1983).
21. R. V. Mehta, R. Patel, R. Desai, R. V. Upadhyay, and K. Parekh, "Experimental evidence of zero forward scattering by magnetic spheres," Phys. Rev. Lett. **96**, 127402 (2006).
22. B. S. Luk'yanchuk , M. I. Tribelsky, Z. B. Wang , Y. Zhou, M. H. Hong , L. P. Shi, T. C. Chong, "Extraordinary scattering diagram for nanoparticles near plasmon resonance frequencies," Appl. Phys. A **89**, 259–264 (2007).
23. Y. H. Fu, A. I. Kuznetsov, A. E. Miroshnichenko, Y. F. Yu, and B. Luk'yanchuk, "Directional visible light scattering by silicon nanoparticles," Nat. Commun. **4**, 1527 (2013).
24. J. M. Geffrin, B. García-Cámara, R. Gómez-Medina, P. Albella, L. S. Froufe-Pérez, C. Eyraud, A. Litman, R. Vaillon, F. González, M. Nieto-Vesperinas, J. J. Sáenz, and F. Moreno, "Magnetic and electric coherence in forward- and back-scattered electromagnetic waves by a single dielectric subwavelength sphere," Nat. Commun. **3**, 1171–1178 (2012).
25. B. Rolly, B. Stout, and N. Bonod, "Boosting the directivity of optical antennas with magnetic and electric dipolar resonant particles," Opt. Express **20**, 20376–20386 (2012).
26. W. D. Zhou, D. Y. Zhao, Y. C. Shuai, H. J. Yang, S. Chuwongin, A. Chadha, J. H. Seo, K. X. Wang, V. Liu, Z. Q. Ma, and S. H. Fan, "Progress in 2D photonic crystal Fano resonance photonics," Prog. Quant. Electron. **38**, 1–74 (2014).
27. J. A. Schuller and M. L. Brongersma, "General properties of dielectric optical antennas," Opt. Express **17**, 24084–24095 (2009).
28. W. D. Luo and X. L. Qi, "Massive Dirac surface states in topological insulator/magnetic insulator heterostructures," Phys. Rev. B **87**, 085431 (2013).
29. A. G. Grushin and F. Juan, "Finite-frequency magnetoelectric response of three-dimensional topological insulators," Phys. Rev. B **86**, 075126 (2012).
30. P. Wei, F. Katmis, B. A. Assaf, H. Steinberg, P. Jarillo-Herrero, D. Heiman, and J. S. Moodera,"Exchange-coupling-induced symmetry breaking in topological insulators," Phys. Rev. Lett. **110**, 186807 (2013).

1. Introduction

Recently, topological insulators (TIs) have been received considerable interest as an emerging phase in condensed matter physics [1–3]. TIs resemble ordinary insulators with a bulk energy gap but possess gapless edge or surface states within the bulk energy gap which are protected by the time-reversal symmetry. This unique feature gives rise to many unusual physical properties. In addition to many exotic electronic and transport properties, a novel quantized topological magneto-electric (TME) effect – an applied electric (magnetic) field can induce magnetic (electric) polarization – has been revealed in TIs [3]. An additional term in the Maxwell Lagrangian, $\Delta\mathscr{L} = (\theta\alpha/4\pi^2)\mathbf{E}\cdot\mathbf{B}$, is introduced to describe the TME effect [3, 4], where $\alpha = e^2/\hbar c$ is the fine structure constant, $\theta = (2p+1)\pi$ is the quantized axion angle [4] with p being an integer, and $\mathbf{E}$ and $\mathbf{B}$ are the electric field and magnetic induction, respectively. The TME effect plays a key role in the electromagnetic (EM) responses of TIs and many unconventional optical phenomena due to the TME effect have been found [5–11].

The scattering of EM waves by small particles is an interesting optical problem and has been treated systematically in the literatures [12, 13] for conventional scatterers. The EM scattering depends strongly on the optical properties of the constituent materials of the scatterers. Owing to the TME effect, EM scattering by TI scatterers should be different from that by conventional ones. Indeed, a parity violating and a strong perturbation of dipole radiation are found in axionic scatterers [14]. In the Rayleigh limit, the quantization of the TME effect can be simply determined by the scattered electric fields in the far field [15]. In this paper, we study theoretically the EM scattering by circular TI cylinders in both the Rayleigh and Mie scattering regimes. Interestingly, strong scattering in the backward direction due to the TME is revealed, which is absent for bi-isotropic [16] (chiral or Tellegen) scatterers since the TME effect is basically a

#223523 - $15.00 USD Received 19 Sep 2014; revised 8 Nov 2014; accepted 20 Nov 2014; published 4 Dec 2014
(C) 2014 OSA

surface effect rather than a bulk one. Moreover, antiresonances for TI cylinders are found in the Mie scattering regime showing an interesting field trapping phenomenon.

2. Scattering coefficients

The propagation of EM waves in a conventional homogeneous medium can be described by the Helmholtz equation $\nabla^2\mathbf{F}+k^2\mathbf{F}=0$, where $\mathbf{F}$ is either the vector field $\mathbf{E}$ or $\mathbf{B}$, k is the corresponding wavevector, ω is the angular frequency, and c is the light speed in vacuum. In TIs, however, the constitutive relations should be modified as [3]

$$\mathbf{D} = \varepsilon\mathbf{E}-\overline{\alpha}\mathbf{B}, \tag{1a}$$

$$\mathbf{H} = \mathbf{B}/\mu+\overline{\alpha}\mathbf{E}, \tag{1b}$$

where $\mathbf{D}$ and $\mathbf{H}$ are respectively the electric displacement and magnetic field, $\overline{\alpha}=\theta\alpha/\pi$ is an odd-numered multiple of α, and ε and μ are respectively the permittivity and permeability. It can be easily verified that, if the modified constitutive relations are applied in the Maxwell equations, the corresponding master equation remains the same form as the one for the topologically trivial case with $\overline{\alpha}=0$. Interestingly, the dispersion relation $k=\sqrt{\varepsilon\mu}\,\omega/c$ is independent of the factor $\overline{\alpha}$. This implies that the TME effect is basically a surface effect, different from chiral media in which the chirality parameter κ enters the corresponding dispersion relation [17]. Therefore, the unusual optical properties of TIs should be contributed from the TI boundaries.

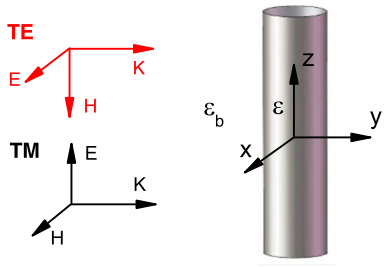

Fig. 1. Schematic view of a circular TI cylinder placed along the z axis. The incident EM wave with TE or TM polarization is propagating along y axis.

The EM scattering by a TI cylinder could be solved by the standard multiple expansion method [15]. The system under study is schematically shown in Fig. 1. In the present work, we consider an EM wave $\mathbf{E}_{\rm inc}=E_0(e_{i\perp}\hat{e}_x-e_{i\parallel}\hat{e}_z)e^{ik_by}$ is incident perpendicular to the cylinder, where E_0 is the amplitude, $k_b=\sqrt{\varepsilon_b\mu_b}\omega/c$ is the wavevector in the background medium. In this configuration, there are two independent polarizations of the incident EM wave: TE (with the electric field perpendicular to the cylinder) and TM (with electric field parallel to the cylinder). Here we use $e_{i\perp}$ and $e_{i\parallel}$ represent the polarization-vector components of the incident wave with $e_{i\perp}=1$ and $e_{i\parallel}=0$ standing for the TE polarization, and $e_{i\perp}=0$ and $e_{i\parallel}=1$ for the TM polarization. Similar to that in conventional circular cylinders, the EM wave functions can be expanded by the vector cylindrical harmonics $\mathbf{M}_n^{(I)}(k\rho,\varphi)$ and $\mathbf{N}_n^{(I)}(k\rho,\varphi)$ [12], in which n is an integer, ρ is the radial distance, φ is the azimuth angle, and I stands for which kind of the Bessel (Hankel) function we use. The scattered electric field and the internal field inside the TI

#223523 - $15.00 USD Received 19 Sep 2014; revised 8 Nov 2014; accepted 20 Nov 2014; published 4 Dec 2014
(C) 2014 OSA

cylinder can be expanded respectively in terms of these vector cylindrical harmonics

$$\mathbf{E}_{\text{sca}} = \sum_{n=-\infty}^{\infty} E_n \left[i a_n \mathbf{M}_n^{(3)} + b_n \mathbf{N}_n^{(3)} \right], \tag{2a}$$

$$\mathbf{E}_{\text{int}} = \sum_{n=-\infty}^{\infty} E_n \left[c_n \mathbf{M}_n^{(1)} + d_n \mathbf{N}_n^{(1)} \right], \tag{2b}$$

where a_n and b_n are the scattering coefficients, $E_n = E_0/k_b$. The superscripts 1 and 3 stand for the Bessel function of the first kind and the Hankel function of the first kind, respectively. Note that the scattering coefficients a_n and b_n are associated with the electric and magnetic multipoles of order n, respectively.

It can be shown that by imposing the standard boundary conditions the scattering coefficients for circular TI cylinders under normal incidence can be found as

$$a_n = \frac{e_{i\perp} A_n D_n + \widetilde{\alpha} f_n}{A_n B_n + \widetilde{\alpha}^2 t_n}, \tag{3a}$$

$$b_n = \frac{e_{i\parallel} B_n C_n + \widetilde{\alpha} g_n}{A_n B_n + \widetilde{\alpha}^2 t_n}, \tag{3b}$$

where $\widetilde{\alpha} = \overline{\alpha}/\sqrt{\varepsilon_b}$ ($\widetilde{\alpha} = \overline{\alpha}$ as the background is vacuum), A_n, B_n, C_n, and D_n are the same functions as defined in circular dielectric cylinders [12]

$$\begin{aligned}
A_n(x) &= m J_n'(mx) H_n^{(1)}(x) - J_n(mx) H_n^{(1)'}(x), \\
B_n(x) &= m J_n(mx) H_n^{(1)'}(x) - J_n'(mx) H_n^{(1)}(x), \\
C_n(x) &= m J_n'(mx) J_n(x) - J_n(mx) J_n'(x), \\
D_n(x) &= m J_n(mx) J_n'(x) - J_n'(mx) J_n(x).
\end{aligned}$$

Here, J_n and $H_n^{(1)}$ are respectively the Bessel and Hankel functions of the first kind , $x = k_b r$ is the size parameter with r being the cylinder radius, and $m = \sqrt{\varepsilon\mu/\varepsilon_b\mu_b}$ is the relative refractive index. In this study we assume all materials are nonmagnetic, i.e., $\mu = \mu_b = 1$. The coefficients related to the internal fields inside the cylinders are

$$c_n = \frac{-i J_n'(x) e_{i\perp} + i H_n^{(1)'}(x) a_n}{m J_n'(mx)}, \tag{4a}$$

$$d_n = \frac{-J_n(x) e_{i\parallel} + H_n^{(1)}(x) b_n}{m J_n(mx)}. \tag{4b}$$

The auxiliary functions f_n, g_n, and t_n with the prefactor $\widetilde{\alpha}$ (or $\widetilde{\alpha}^2$) are unique in TI cylinders due to the TME effect, given by

$$\begin{aligned}
f_n(x) &= J_n(mx) J_n'(mx) \left[-e_{i\parallel} \frac{2i}{\pi x} + \widetilde{\alpha} e_{i\perp} J_n'(x) H_n^{(1)}(x) \right], \\
g_n(x) &= J_n(mx) J_n'(mx) \left[-e_{i\perp} \frac{2i}{\pi x} + \widetilde{\alpha} e_{i\parallel} J_n(x) H_n^{(1)'}(x) \right], \\
t_n(x) &= J_n(mx) J_n'(mx) H_n^{(1)}(x) H_n^{(1)'}(x).
\end{aligned}$$

It can be verified that $a_n = a_{-n}$ and $b_n = b_{-n}$, similar to those in conventional cylinders [12]. Note that a_n and b_n are polarization dependent and there hence exist two independent sets,

#223523 - $15.00 USD Received 19 Sep 2014; revised 8 Nov 2014; accepted 20 Nov 2014; published 4 Dec 2014
(C) 2014 OSA

$\{a_{n,\mathrm{TE}}, b_{n,\mathrm{TE}}\}$ and $\{a_{n,\mathrm{TM}}, b_{n,\mathrm{TM}}\}$ for TE and TM polarizations, respectively. For TI cylinders, we have another identity $a_{n,\mathrm{TM}} = b_{n,\mathrm{TE}}$ which can be easily verified. For topological-trivial insulators, the corresponding axion angle $\theta = 0$ and the scattering coefficients are reduced to the conventional ones given in [12]. Compared with ordinary dielectric cylinders, extra contributions resulting from the TME effect appear in both $\{a_n\}$ and $\{b_n\}$ [18, 19], leading to many unusual scattering properties. For example, for an ordinary dielectric cylinder a TE incident wave cannot excite the magnetic multipoles because $b_{n,\mathrm{TE}} = 0$ (not valid for $b_{n,\mathrm{TM}}$ generally). However, for a TI cylinder, $b_{n,\mathrm{TE}}$ does not vanish in general, implying that the magnetic multipoles can be excited. The scattering efficiency defined by $Q(\theta) = \frac{2}{x}\sum_{n=-\infty}^{\infty}\{|a_n|^2 + |b_n|^2\}$ is now a function of θ. To estimate the weight of the scattering efficiency contributed from the TME effect, we define a relative scattering efficiency, $Q_r = [Q(\theta \neq 0) - Q(\theta = 0)]/Q(\theta = 0)$, where $Q(\theta \neq 0)$ and $Q(\theta = 0)$ are the scattering efficiency with an axion angle $\theta \neq 0$ and $\theta = 0$, respectively.

3. Unusual scattering pattern

To obtain the fields of scattered waves in the far field, an amplitude scattering matrix T is usually introduced which relates the electric field of the scattered wave to that of incident wave [12]

$$\begin{bmatrix} E_{s\|} \\ E_{s\perp} \end{bmatrix} = e^{i3\pi/4}\sqrt{\frac{2}{\pi k\rho}}e^{ik\rho}\begin{bmatrix} T_1 & T_4 \\ T_3 & T_2 \end{bmatrix}\begin{bmatrix} E_{i\|} \\ E_{i\perp} \end{bmatrix}, \tag{5}$$

where $E_\|$ and $E_\perp$ are the electric-field components parallel and perpendicular to the cylinder, respectively; the subscripts i and s stand for the incident and scattered wave, respectively; and T_i ($i = 1, 2, 3, 4$) are the elements of amplitude scattering matrix defined by

$$T_1 = \sum_{n=-\infty}^{\infty} e^{-in\phi} b_{n,\mathrm{TM}}, \tag{6a}$$

$$T_2 = \sum_{n=-\infty}^{\infty} e^{-in\phi} a_{n,\mathrm{TE}}, \tag{6b}$$

$$T_3 = \sum_{n=-\infty}^{\infty} e^{-in\phi} a_{n,\mathrm{TM}}, \tag{6c}$$

$$T_4 = \sum_{n=-\infty}^{\infty} e^{-in\phi} b_{n,\mathrm{TE}}. \tag{6d}$$

Here, $\phi = \pi/2 - \varphi$ is the scattering angle [15]. From the electric field of the scattered wave, we can obtain easily its intensity. The intensity of the scattered wave I can be decomposed as two components according to the polarizations, one parallel and the other perpendicular to the cylinder, given by

$$I_\| = |E_\||^2 = \frac{2}{\pi k\rho}\left|T_1 e_{i\|} + T_4 e_{i\perp}\right|^2, \tag{7}$$

$$I_\perp = |E_\perp|^2 = \frac{2}{\pi k\rho}\left|T_3 e_{i\|} + T_2 e_{i\perp}\right|^2, \tag{8}$$

where we assume that the incident plane wave has a unit intensity.

We first discuss the scattering in the Rayleigh scattering limit ($x, mx \ll 1$). With the known

#223523 - $15.00 USD Received 19 Sep 2014; revised 8 Nov 2014; accepted 20 Nov 2014; published 4 Dec 2014
(C) 2014 OSA

scattering coefficients [15], the intensity for the TE incident wave can be obtained as

$$I_{\parallel,\mathrm{TE}} = \frac{2}{k\rho}\pi x^4 \left| \frac{\widetilde{\alpha}}{4} - \frac{\widetilde{\alpha}\cos\phi}{2m^2+2+\widetilde{\alpha}^2} \right|^2, \tag{9a}$$

$$I_{\perp,\mathrm{TE}} = \frac{2}{k\rho}\pi x^4 \left| \frac{(2m^2-2+\widetilde{\alpha}^2)\cos\phi}{2(2m^2+2+\widetilde{\alpha}^2)} \right|^2. \tag{9b}$$

Note that $I_{\parallel,\mathrm{TE}}$ should vanish for conventional cylinders. For TI cylinders, however, the contributions from the magnetic monopolar and dipolar terms induced by the TME effect lead to a non-zero $I_{\parallel,\mathrm{TE}}$. Interestingly, the scattered fields from the magnetic monopole and dipole interfere destructively in forward direction ($\phi = 0^\circ$), while constructively in the backward direction ($\phi = 180^\circ$). In contrast, $I_{\perp,\mathrm{TE}}(\phi)$, which is contributed from the electric dipolar term induced by the bulk, has the same magnitude in both the forward and backward directions. In general cases, the intensity of the scattered wave is dominated by $I_{\perp,\mathrm{TE}}$ since $\widetilde{\alpha}$ is very small. In the case of $m \sim 1$ (the refractive index of the TI cylinder is very close to that of the background), however, the scattering from the bulk is negligibly small such that $I_{\parallel,\mathrm{TE}} \gg I_{\perp,\mathrm{TE}}$. The scattering by TI cylinders is now dominated by $I_{\parallel,\mathrm{TE}}$, leading to strong scattering in the backward direction. In fact, the ratio of the backward-to-forward scattering intensity takes a large value ($\sim 1/\widetilde{\alpha}^2$) as $m \sim 1$.

For the TM incident wave, the intensity components of the scattered wave are given by

$$I_{\parallel,\mathrm{TM}} = \frac{2}{k\rho}\pi x^4 \left| \frac{m^2-1+\widetilde{\alpha}^2}{4} - \frac{\widetilde{\alpha}^2\cos\phi}{2(2m^2+2+\widetilde{\alpha}^2)} \right|^2, \tag{10a}$$

$$I_{\perp,\mathrm{TM}} = \frac{2}{k\rho}\pi x^4 \left| \frac{\widetilde{\alpha}}{4} - \frac{\widetilde{\alpha}\cos\phi}{2m^2+2+\widetilde{\alpha}^2} \right|^2. \tag{10b}$$

Obviously, $I_{\parallel,\mathrm{TM}}$ is mainly from the monopolar term of the scattered wave by the bulk. However, $I_{\perp,\mathrm{TM}}$ has the similar property as $I_{\parallel,\mathrm{TE}}$, showing the interesting destructive interference in the forward direction and constructive interference in the backward direction. As $m \sim 1$, we have $I_{\parallel,\mathrm{TM}} \ll I_{\perp,\mathrm{TM}}$, manifesting strong scattering in the backward direction. The ratio of the backward-to-forward scattered intensity also takes a large value in order of $1/\widetilde{\alpha}^2$ as $m \sim 1$. Note that Rayleigh scattering in conventional dielectric cylinders displays a symmetric scattering pattern in forward and backward directions. Thus, the strong backward scattering in TI cylinders stem from the TME effect.

From the above discussions, the key to realizing strong backward scattering is to suppress the contribution of bulk scattering. The choice of $m \sim 1$ can indeed eliminate the bulk scattering to attain strong backward scattering. But it is rather difficult to realize experimentally. Practically, we can adopt instead a hollow TI cylinder to implement strong backward scattering as shown in Fig. 2. The axion angles for the hollow TI cylinder should be properly chosen since there are two interfaces. We assume that the axion angle of the hollow TI cylinder is $(2p+1)\pi$, whereas the axion angle of the vacuum outside and inside the hollow cylinder is respectively 0 and $(2p+1)2\pi$, as in [7] for TI thin films. Although the axion angles 0 and $(2p+1)2\pi$ are equivalent in the topological sense, this proper choice guarantees that the surface currents at the two interfaces do not cancel each other.

In Fig. 2(a), we calculate the relative scattering efficiency $|Q_r|$ for the hollow cylinder. The outer radius and the wall thickness of the hollow cylinder are denoted by r_0 and d_0, respectively. It can be observed from Fig. 2(a) that $|Q_r|$ decreases with increasing $d(= d_0/r_0)$, indicating that the bulk scattering increases with d. However, for small d (< 0.001) the scattering efficiency from the TME effect is manifest in both the Rayleigh (e.g., $x = 0.05$) and Mie (e.g., $x = 1$)

#223523 - $15.00 USD Received 19 Sep 2014; revised 8 Nov 2014; accepted 20 Nov 2014; published 4 Dec 2014
(C) 2014 OSA

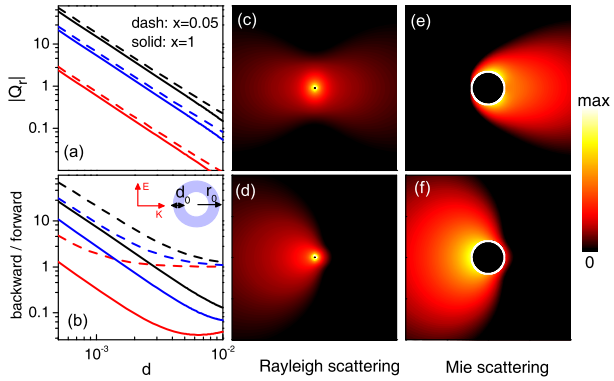

Fig. 2. Scattering of TE incident waves by a hollow TI cylinder with $\varepsilon = 30$. The background is vacuum with $\varepsilon_b = 1$. The cross-sectional profile of the hollow cylinder is shown in the inset of (b). (a) $|Q_r|$ as a function of the thickness parameter $d = d_0/r_0$. Here, $x = k_b r_0$ is the size parameter. (b) Ratio of the scattered radiant intensities I between the backward and forward directions. In (a) and (b), the red, blue and black curves correspond to the hollow TI cylinder with the axion angle $\theta = \pi$, 3π and 5π, respectively. (c)–(f) Field distributions $|E|^2$ of the scattered waves for $d = 0.001$. In (c) and (e), the axion angle of the cylinder is 0, standing for a conventional dielectric hollow cylinder; whereas in (d) and (f) the axion angle is 5π, standing for a TI hollow cylinder. In (c) and (d), $x = 0.05$; and in (e) and (f), $x = 1$.

scattering regimes. For small d, the intensity of the backward scattering can surpass the forward scattering in both the Rayleigh and Mie scattering regimes, as can be seen from Fig. 2(b), especially for large axion angles. Figures 2(c)-2(f) show the field distributions of the scattered EM wave. Obviously, the conventional hollow cylinder ($\theta = 0$) displays an almost symmetric scattering pattern in the backward and forward directions in the Rayleigh scattering regime. In the Mie scattering regime, the scattering pattern shows strong forward scattering. The symmetric and forward scattering in respectively the Rayleigh and Mie scattering regimes is the known features for conventional dielectric scatterers. For a TI hollow cylinder with a small wall thickness, however, both the Rayleigh and Mie scattering show a pattern of strong backward scattering. For TM incident waves, similar results are also observed (data not shown).

The underlying physics for the strong backward scattering in TI hollow cylinders can be understood by the interference between electric and magnetic multipoles. Note that such backward scattering has also been found in other kinds of scatterers such as magnetic [20, 21], metallic [22], or semiconducting [23–25] particles. To achieve strong backward scattering in magnetic spheres, the optical constants should satisfy the condition $\varepsilon = (4-\mu)/(2\mu+1)$ [20]. Under this condition, the radiation fields from the induced electric and magnetic dipoles have the same strength but are out of phase in the forward direction and in phase in the backward direction. For metallic spheres [22] or semiconducting spheres [23–25], the strong backward scattering is frequency-dependent. The magnetic dipole moment arising from the closed loops of the induced displacement currents are usually caused by resonances. As a result, the observed strong backward scattering exists only in a narrow frequency range. In hollow TI cylinders with a small wall thickness, the interference between the electric and magnetic multipoles is constructive in the backward direction and destructive in the forward direction, eventually leading to strong backward scattering. Note that the frequency range for the strong backward scattering is wide since the TME effect is a non-resonant effect. Moreover, such strong backward scattering can occur not only in Rayleigh scattering but also in Mie scattering.

#223523 - $15.00 USD Received 19 Sep 2014; revised 8 Nov 2014; accepted 20 Nov 2014; published 4 Dec 2014
(C) 2014 OSA

4. Antiresonances

In Fig. 3, the scattering coefficients of the four lowest order modes for a TI cylinder in vacuum as a function of the size parameter x for TE incident waves are shown. Obviously, there exist resonances and *antiresonances* in both $a_{n,\mathrm{TE}}$ and $b_{n,\mathrm{TE}}$. Physically, a_n and b_n are associated with the n-th order electric and magnetic multiplolar modes, respectively. The resonances at $x = 0.425$ in $|a_{0,\mathrm{TE}}|$ and $x = 0.670$ in $|a_{1,\mathrm{TE}}|$ correspond to the excitation of the electric monopolar and dipolar modes, respectively. In contrast, at the antiresonances ($x = 0.946$ in $|a_{0,\mathrm{TE}}|$ and $x = 0.727$ in $|a_{1,\mathrm{TE}}|$) no such electric monopolar and dipolar modes can be excited since at these particular x the corresponding scattering coefficients are almost zero. The asymmetric lineshapes in Fig. 3 can be explained by the interference between the resonant and direct scattering similar to the cases considered in [26].

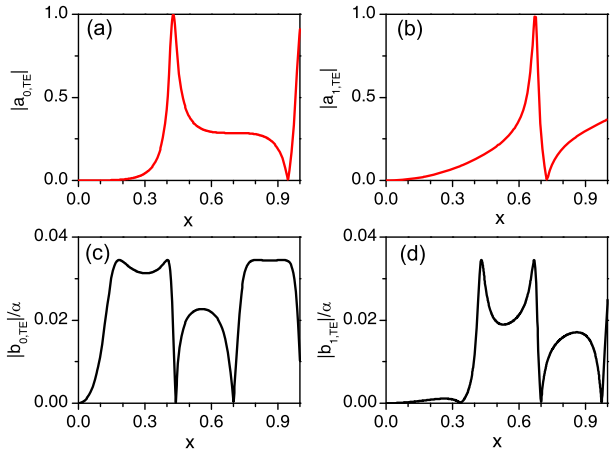

Fig. 3. Scattering coefficients a_n and b_n as functions of the size parameter x with $n = 0, 1$ for the TE incident wave. The dielectric constant of the TI cylinder is $\varepsilon = 30$ and its axion angle is π. The background medium is vacuum.

The scattering coefficients $a_{n,\mathrm{TE}}$ of a TI cylinder should be similar to those of a dielectric cylinder with the same refractive index [27] since the fine structure constant is much smaller than one. As a result, the TME effect could not be manifest in $a_{n,\mathrm{TE}}$. However, it emerges in $b_{n,\mathrm{TE}}$ since $b_{n,\mathrm{TE}}$ should vanish in conventional dielectric cylinders. Interestingly, there exist also resonances and antiresonances in $b_{n,\mathrm{TE}}$. Right at these antiresonances, the corresponding scattering coefficients vanish. In order to enable $b_{n,\mathrm{TE}} = 0$, the function g_n in Eq. (3) should be zero, or in other words, the condition $J_n(mx)J_n'(mx) = 0$ should be satisfied. Therefore, the antiresonances correspond exactly to the roots of $J_n(mx) = 0$ or $J_n'(mx) = 0$. At the antiresonances, all the introduced auxiliary functions that are related to the TME effect should be zero, namely, $f_n = g_n = t_n = 0$. The scattering now is reduced to the one for conventional dielectric cylinders, implying the absence of the TME effect. For TM polarization, similar conclusions can be drawn since $a_{n,\mathrm{TM}} = b_{n,\mathrm{TE}}$.

To verify our analysis, we show in Fig. 4 the field distributions for two antiresonances at $x = 0.439$ and 0.336, corresponding to $J_0(mx) = 0$ and $J_1'(mx) = 0$, or $b_{0,\mathrm{TE}} = 0$ and $b_{1,\mathrm{TE}} = 0$, respectively. For TE incident waves, from the definition of the vector cylindrical harmonics $\mathbf{M}_n$ and $\mathbf{N}_n$, the electric filed component E_φ and the magnetic induction component B_z are proportional to $J_n'(mx)$ and $J_n(mx)$, respectively. For the magnetic monopole mode at $x = 0.439$, it is obvious that $B_z = 0$ at the boundary since $J_0(mx) = 0$. Inside the TI cylinder, E_φ is nonzero which can induce a nonzero B_φ inside the cylinder via the TME effect. However, the com-

#223523 - $15.00 USD Received 19 Sep 2014; revised 8 Nov 2014; accepted 20 Nov 2014; published 4 Dec 2014
(C) 2014 OSA

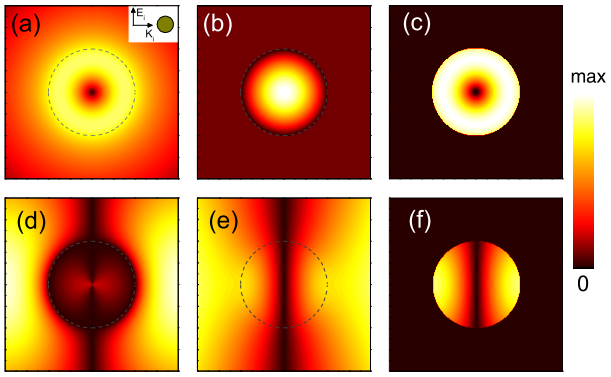

Fig. 4. Field distributions at two antiresonances $x = 0.439$ (upper panels) and 0.336 (lower panels). (a) and (d) are for $|E_\varphi|$, (b) and (e) for $|B_z|$, (c) for $|B_\varphi|$, and (f) for $|D_z|$. The boundary of the TI cylinder is indicated by dashed lines.

ponents of the scattered fields H_φ and B_ρ should be zero since $b_{0,\mathrm{TE}} = 0$. The magnetic field component B_φ is not continuous at the boundary. Interestingly, B_φ is completely trapped inside the cylinder. For the magnetic dipole mode at $x = 0.336$, $E_\varphi = 0$ at the boundary since it corresponds to $J_1'(mx) = 0$. As a result, H_φ cannot be induced inside the cylinder by the TME effect. However, D_z can be induced by the TME effect since B_z inside the cylinder may not be zero. Similar to B_φ for the monopole mode, D_z for the dipole mode is trapped completely inside the cylinder.

The vanishment of the field component E_φ or B_z at antiresonances for TE incident waves is an exotic phenomenon in TI cylinders and is also a strong evidence that the TME effect is intrinsically a surface effect. For TM incident waves, similar antiresonances also exist. The corresponding vanishing field component at the boundary is now B_φ or E_z instead. The field trapping of B_z or D_φ inside the cylinder can also be observed. For conventional dielectric cylinders, the scattering coefficients a_n and b_n also possess antiresonances at particular size parameters. However, the cylinder is perfectly transparent to the $n-$th harmonic of the incident wave at any antiresonance [27]. There is no such a field trapping phenomenon in conventional dielectric cylinders.

A few points should be mentioned. First, one should introduce a thin magnetic layer coating on the TI surface to open up a surface energy gap E_g [3, 28]. With this magnetic layer, the time reversal symmetry is broken at the surface and the value of θ can be specified definitely. For a typical value $E_g \sim 10$ meV, the corresponding EM wavelength λ_g is about 0.12 mm, the incident wavelength λ should be much larger than λ_g, i.e. $\lambda_g \ll \lambda$, which can be attained with microwaves. Second, if the TI is doped, the doping level we considered should in the gap [29]. Therefore the axion angle is quantized and the "axion electrodynamics" can be applied to describe the EM responses of the system. Third, the role that the magnetic layer plays in the EM scattering should be rigorously restricted in the total EM scattering. Since the magnetic layer can be as thin as several nanometers [30], the optical distance of this layer is extremely small in the microwave regime.

5. Conclusion

In summary, we study systematically the EM scattering properties of circular TI cylinders. Owing to the TME effect, scattering in TI cylinders shows unusual feathers. For TI cylinders with a refractive index close to that of the background or for hollow TI cylinders with a small

#223523 - $15.00 USD Received 19 Sep 2014; revised 8 Nov 2014; accepted 20 Nov 2014; published 4 Dec 2014
(C) 2014 OSA

wall thickness with respect to the wavelength, strong backward scattering are found in both the Rayleigh and Mie scattering regimes, which is completely different from conventional dielectric cylinders. The underlying physics for the strong backward scattering can be understood by the interference between electric and magnetic multipoles, which are destructive in the forward direction and constructive for the backward scattering. For conventional media, the spectral responses of magnetic dipoles are usually narrow-band since they are caused by resonances in general. However, the enhanced backscattering for TIs is a broadband effect for the non-resonant nature of TME effect. Interesting antiresonances are found showing a field-trapping phenomenon, which does not exist in conventional dielectric cylinders. At anti-resonances, the EM fields generated by the surface Hall currents are completely trapped inside the cylinder.

Acknowledgments

This work is supported by the 973Program (Grant Nos. 2013CB632701 and 2011CB922004). The research of H.D.Z., X.H.L. and J.Z. is further supported by the National Natural Science Foundation of China (Grant No. 11304038 and 11234010). The work of H.D.Z is also supported by the Fundamental Research Funds for the Central Universities (Grant no. CQDXWL-2014-Z005).

#223523 - $15.00 USD Received 19 Sep 2014; revised 8 Nov 2014; accepted 20 Nov 2014; published 4 Dec 2014
(C) 2014 OSA